KEK-CP-088

QED Radiative Corrections to the Non-annihilation Processes Using the Structure Function and the Parton Shower

Y. Kurihara, J. Fujimoto, Y. Shimizu
High Energy Accelerator Research Organization,
Oho 1-1, Tsukuba, Ibaraki 305-0801, Japan

K. Kato, K. Tobimatsu
Kogakuin University, Shinjuku, Tokyo 163-8677, Japan

T. Munehisa
Yamanashi University, Kofu, Yamanashi 400-8510, Japan

Abstract

Inclusion of the QED higher order radiative corrections in the two-photon process, $e^+e^- \to e^+e^-\mu^+\mu^-$, is examined by means of the structure function and the parton shower. Results are compared with the exact $O(\alpha)$ calculations and give a good agreement. These two methods should be universally applicable to any other non-annihilation processes like the single-W productions in the e^+e^- collisions. In this case, however, the energy scale for the evolution by the renormalization-group equation should be chosen properly depending on the dominant diagrams for the given process. A method to find the most suitable energy scale is proposed.

1 Introduction

A precise prediction of the cross sections for high-energy e^+e^- scattering frequently requires an estimation of the radiative corrections beyond the lowest order calculations. Among various corrections from the electro-weak interactions it is known that the QED radiative corrections to the initial-state particles gives the greatest contribution in general. Sometimes all order summation is necessary to give the needed precision. In the leading-logarithmic approximation the higher-order summation of the QED corrections can be done easily thanks to the factorization theorem. The theorem given by ref.[1] guarantees that the final state corrections result only a small contribution to the total cross section.

For the e^+e^- annihilation processes we have tools. They are universally applicable because only the initial-state QED corrections are involved; the structure function[2] and the parton shower[3, 4] methods widely used in high energy physics today. The recent experiments, however, require the higher order corrections for the multi-particle final states, such as the four-fermion productions at LEP2. Even though the exact calculations of the higher order corrections are very difficult or impossible, still it is possible to include the biggest QED corrections by making use of those tools as long as the process is dominated by the annihilation.

On the other hand for the non-annihilation processes it has been not well investigated how to apply these tools. Only a few examples are the Bhabha scattering to which the structure function has been used in[5] and the parton shower in[6]. In the present work it will be shown that the structure function and the parton shower can be also the universal tools for any non-annihilation process once the evolution energy is settled.

First we apply and examine both methods to the two-photon process, $e^+e^- \to e^+e^-\mu^+\mu^-$ in the next section. The obtained total and differential cross sections are compared with those given by the $O(\alpha)$ corrections[9] in section 3. These methods must be universal to any process, again thanks to the factorization theorem. The energy scale, however, with which the radiative correction is evolved should be carefully chosen for the non-annihilation processes. An unique and definite way to find this energy scale is explained in section 4.

2 Calculation method

2.1 Structure Function Method

The structure function(SF) for the initial state radiative correction(ISR) is well established for the case of the e^+e^- *annihilation* processes. The observed cross section corrected by ISR can be expressed by using SF as

$$\sigma_{total}(s) = \int^1 dx_1 \int^1 dx_2 D_{e^-}(x_1,s) D_{e^+}(x_2,s) \sigma_0(x_1 x_2 s), \tag{1}$$

where $D_{e^\pm}(x,s)$ is the electron(positron) structure function with $x_{1,2}$ being the energy fractions of $e^\pm$. The SF up to the $O(\alpha^2)$ is given by[7]

$$\begin{aligned} D(x,s) &= \frac{\beta}{2}(1-x)^{\frac{\beta}{2}-1}\left[1+\frac{3}{8}\beta+\beta^2\left(\frac{9}{128}-\frac{\pi^2}{48}\right)\right]-\frac{\beta}{4}(1+x) \\ &+ \left(\frac{\beta}{4}\right)^2\left[2(1+x)\mathtt{ln}\frac{1}{1-x}-\frac{1+3x^2}{2(1-x)}\mathtt{ln}x-\frac{5+x}{2}\right], \qquad (2) \\ \beta &= \frac{2\alpha}{\pi}\left(\mathtt{ln}\frac{s}{m_e^2}-1\right). \qquad (3) \end{aligned}$$

In deriving this formula, which is given by solving the Altarelli-Parisi equation in the LL approximation[8], we have used an *ad hoc* trick to get more accuracy. The factor $\beta = (2\alpha/\pi)\mathtt{ln}(s/m_e^2)$ is replaced by $\beta = (2\alpha/\pi)(\mathtt{ln}(s/m_e^2)-1)$ to match with the perturbative calculations.

Let us apply the SF method to the two-photon process,

$$e^-(p_-)+e^+(p_+) \;\rightarrow\; e^-(q_-)+e^+(q_+)+\mu^-(k_-)+\mu^+(k_+). \tag{4}$$

For the forward scattering of $e^\pm$, the multi-peripheral diagrams shown in Fig.1 give the dominant contribution to the total cross section. Thus only the multi-peripheral diagrams are taken into account in this work. In this case the corrected cross section is given by

$$\begin{aligned} \sigma_{total}(s,t_\pm) &= \int dx_{I-}\int dx_{F-}\int dx_{I+}\int dx_{F+} D_{e^-}(x_{I-},Q_-^2) D_{e^-}(x_{F-},Q_-^2) \\ &\quad D_{e^+}(x_{I+},Q_+^2) D_{e^+}(x_{F+},Q_+^2)\sigma_0(\hat{s},\hat{t}_\pm). \qquad (5) \end{aligned}$$

Here $Q_\pm^2$ is the energy scale to be fixed, with which SF should be driven. Since these functions are common to the initial and the final radiations from

the $e^{\pm}$'s in the leading-logarithmic(LL) approximation, we shall drop the subscript $e^{\pm}$ from the SF hereafter. After(before) the photon radiation the initial(final) momenta $p_{\pm}$ ($q_{\pm}$) become $\hat{p}_{\pm}$ ($\hat{q}_{\pm}$) in the following ways

$$\hat{p}_- = x_{I-}p_-, \quad \hat{q}_- = \frac{1}{x_{F-}}q_-, \tag{6}$$

$$\hat{p}_+ = x_{I+}p_+, \quad \hat{q}_+ = \frac{1}{x_{F+}}q_+, \tag{7}$$

respectively. Then the CM energy squared($s = (p_- + p_+)^2$) and the momentum transfer squared($t_{\pm} = (p_{\pm} - q_{\pm})^2$) are scaled as follows,

$$\hat{s} = x_{I-}x_{I+}s, \quad \hat{t}_{\pm} = \frac{x_{I\pm}}{x_{F\pm}}t_{\pm}. \tag{8}$$

Note that SF behaves like $\delta(1-x)$ when $\beta \to 0$, that is,

$$\begin{aligned}\int_0^1 dx\frac{\beta}{2}(1-x)^{\frac{\beta}{2}-1}f(x) &= f(1) + \int_0^1 dx\Big[(1-x)^{\frac{\beta}{2}} - 1\Big]f'(x) \\ &= f(1) + \frac{\beta}{2}\int_0^1 dx\mathtt{ln}(1-x)f'(x) + O(\beta^2),\end{aligned} \tag{9}$$

where $f(x)$ is an arbitrary smooth function.

The choice of the energy scale in SF is not a trivial matter. As pointed out in Ref.[11] it is natural to use $-t_{\pm}$ instead of s for the two-photon processes. The justification of this choice is given by comparing them with the perturbative calculations. This could be done in the region where the soft-photon approximation of the total cross section is valid. Since the corrections for the e^- and e^+ sides must be symmetric, it is enough to consider only those from the e^- side. The total correction will be obtained by doubling them. Then Eq.(5) can be simplified as

$$\sigma(s) = \int dx_I \int dx_F D(x_I, Q^2)D(x_F, Q^2)\sigma_0(x_I s). \tag{10}$$

The integrations are performed in the region $1 - x_{I,F} \ll 1$. Since the Born cross section of this process($\sigma_0(\hat{s})$) is a smooth function of $\hat{s}$, the cross section in the soft photon approximation is written as

$$\sigma_{soft} = \sigma_0(s)\int_{1-\frac{k_c}{E}}^1 dx_I \int_{(1-\frac{k_c}{E})/x_I}^1 dx_F D(x_I, Q^2)D(x_F, Q^2)$$

$$= \sigma_0(s)\int_0^{\frac{k_c}{E}} dy H(y,Q^2), \tag{11}$$

$$H(y,Q^2) = \int_{1-y}^1 \frac{dx_F}{x_F} D(x_F,Q^2) D\left(\frac{1-y}{x_F},Q^2\right), \tag{12}$$

where k_c is the maximum energy of the sum of the initial and the final photon energies and $E = p^0 \approx q^0$. The function H is called *radiator* and can be obtained easily from SF as

$$\begin{aligned} H(x,s) &= D(1-x,s)|_{\beta\to 2\beta} \\ &= \beta x^{\beta-1}\left[1+\frac{3}{4}\beta+\frac{\beta^2}{4}\left(\frac{9}{8}-\frac{\pi^2}{3}\right)\right]-\beta\left(1-\frac{x}{2}\right) \\ &+ \frac{\beta^2}{8}\left[-4(2-x)\ln x-\frac{1+3(1-x)^2}{x}\ln(1-x)-6+x\right]. \end{aligned} \tag{13}$$

The integration of the function H in the small k_c/E region gives

$$\int_0^{\frac{k_c}{E}} dy H(y,Q^2) = 1+\frac{\alpha}{\pi}\left[-2l(L-1)+\frac{3}{2}(L-1)\right]+O(\alpha^2), \tag{14}$$

where $L = \ln(Q^2/m_e^2)$, and $l = \ln(E/k_c)$. Then the cross section in the soft photon approximation up to the $O(\alpha)$ is obtained,

$$\sigma_{soft} = \sigma_0(s)\left\{1+\frac{\alpha}{\pi}\left[-2l(L-1)+\frac{3}{2}(L-1)\right]\right\}. \tag{15}$$

This expression is compared with the perturbative calculation given by Berends, Daverveldt and Kleiss[9](BDK hereafter). In the BDK program the multi-peripheral diagrams and their $O(\alpha)$ corrections of the self-energy correction to $e^{\pm}$, the vertex correction for $e^{\pm}$-$e^{\pm}$-γ vertex, the soft- and hard-photon emissions and the vacuum polarization of the virtual photons are calculated. The corrections from the photon bridged between different charged lines are not given because the contributions from the box diagrams with photon exchange between e^+ and e^- is known to be small[10]. The LL approximation of the virtual correction factors(vertex + soft photon) is

$$2\mathrm{Re}F_1+\delta_s \to \frac{\alpha}{\pi}\left(-2l(L_t-1)+\frac{3}{2}L_t-2\right), \tag{16}$$

where $L_t = \ln(-t/m_e^2)$ and $t = (p_- - q_-)^2$. By comparing Eqs.(15) and (16) one concludes that the energy scale of SF should be $Q^2 = t$

This comparison shows that once the proper energy scale is found the SF can reproduce the correct evolution of the soft-photon emission along the electron line up to the $O(\alpha)$. However, there remains some mismatch with the constant term. This can be compensated by multiplying an overall factor to the SF. This factor is usually called *K-factor*. When the SF is evolved with $-t$ this factor is found to be $1-\alpha/2\pi$. Then the total *K-factor* for both e^+ and e^- must be $1 - \alpha/\pi$.

It should be noted that the assumption $-t/m_e^2 \gg 1$ does not hold for the forward scattering of the two-photon process. The LL-terms in the SF are no more leading if this happens. To find the region where the approximation is valid the LL terms of the form factor F_1 is compared with the exact form given by `BDK` in Fig.2. While they agree well at high Q^2 region as expected, they show a large deviation in the region $Q^2/m_e^2 < 10$. In order to make SF well-defined, the energy evolution must be truncated at some point, say $L = 1$.

2.2 Parton Shower Method

Instead of the analytic formula of the structure function, a Monte Calro method based on the parton shower algorithm in QED (`QEDPS`) can be used to solve the Altarelli-Parisi equation in the LL approximation[8]. The detailed algorithm of the `QEDPS` is found in Ref.[4] for the e^+e^- annihilation processes and in Ref.[6] for the Bhabha process. For the two-photon process the energy scale for the parton shower evolution is also $-t$. The truncation at $L = 1$ is again imposed. One difference between SF and `QEDPS` is that the *ad hoc* replacement $L \to L - 1$, which was realized by hand for SF, cannot be done for `QEDPS`. This causes a deviation of the *K-factor* from the SF method. The *K-factor* for `QEDPS` is given by $1 - 4\alpha/\pi$. Another significant difference between these two is that `QEDPS` can treat the transverse momentum of emitted photons correctly by imposing the exact kinematics at the $e \to e\gamma$ splitting. It does not affect the total cross sections so much when the final $e^\pm$ have no cut. However, the finite recoiling of the final $e^\pm$ may result a large effect on the tagged cross sections as shown below.

In return to the the exact kinematics at the $e \to e\gamma$ splitting, $e^\pm$ are no more on-shell after photon emission. On the other hand the matrix element

of the hard scattering process must be calculated with the on-shell external particles. A trick to map the off-shell four-momenta of the initial $e^{\pm}$ to those at on-shell is needed. Following method is used in the calculations.

1. $\hat{s} = (\hat{p}_- + \hat{p}_+)^2$ is calculated, where $\hat{p}_\pm$ are the four-momenta of the initial $e^{\pm}$ after the photon emission by `QEDPS`. $\hat{s}$ can be positive even for the off-shell $e^{\pm}$. (When $\hat{s}$ is negative, that event is discarded.)

2. All four-momenta are generated in the rest-frame of the initial $e^{\pm}$ after the photon emission. Four-momenta of the initial $e^{\pm}$ in this frame are $\tilde{p}_\pm$, where $\tilde{p}_\pm = m_e^2$ (on-shell) and $\hat{s} = (\tilde{p}_- + \tilde{p}_+)^2$

3. All four-momenta are rotated and boosted to match the three-momenta of $\tilde{p}_\pm$ with those of $\hat{p}_\pm$.

This method respects the direction of the final $e^{\pm}$ rather than the CM energy of the collision. The total energy does not conserve because of the virtuality of the initial $e^{\pm}$.

3 Numerical Calculations

3.1 No-cut Case

First the total cross section of $e^+e^- \to e^+e^-\mu^+\mu^-$ without any experimental cut is considered. The exact matrix element is generated by the `GRACE` system[12]. Only the multi-peripheral diagrams are generated for the test of the approximation methods. The phase-space integration of the matrix element squared is carried out numerically by `BASES`[13] using an adaptive Monte Calro method. It is trivially confirmed that the Born cross sections agree with `BDK` results within the statistical error of the numerical integration.

The convolution of SF or `QEDPS` with the Born cross section is not a straightforward task because of the complicated four-body kinematics. For a simple two-body process such as the Bhabha scattering the momentum transfer($-t$) can be taken as one of the integration variables and the Eq.(5) will be easily performed then. It is, however, practically impossible to use this technique for the case of the four-body kinematics. Hence we have to admit the following approximation:

1. Eight random numbers obtained from BASES correspond to the eight independent variables of the phase-space integration.

2. All the kinematical variables are determined with *no* radiative effect. The $-t_{\pm}$'s are fixed also.

3. The radiative correction factors of Eq.(5) are determined from $-t_{\pm}$'s, x_{I-} and x_{I+}.

4. A new CM energy is obtained by the fixed x_{I-} and x_{I+}.

5. All the kinematical variables are re-calculated from the same set of the random numbers and the new CM energy.

In this method the evolution energy scale of the radiator is not exactly the same after the re-calculation with the new CM-energy. However, this difference must be beyond the LL order.

The total cross sections without any experimental cuts with SF and QEDPS are summarized in Table 1. The BDK program also includes the correction from the vacuum polarization of the photon propagator. In order to compare the SF and QEDPS results with BDK, this correction is removed. After including the *K-factor* the results of our two methods are in good agreement with the $O(\alpha)$ calculation(without the vacuum polarization).

E_{CM} (GeV)	σ_0 (nb)	$\sigma_{\texttt{sf}}$ (nb)	$\sigma_{\texttt{QEDPS}}$ (nb)	$\sigma_{\texttt{BDK}}$ (nb)
20	97.0(1)	96.3(1)	96.0(2)	96.0(1)
40	137.5(3)	136.3(1)	135.9(3)	135.9(1)
100	202.8(4)	201.0(2)	200.5(4)	200.5(2)
200	262.0(6)	259.8(3)	259.1(6)	258.8(2)

Table 1: Total cross sections without the vacuum correction. σ_0 is the tree cross section. Last column shows the results by the BDK program with the vertex correction, the soft-photon correction and the hard-photon emission. The vacuum polarization is removed from BDK. The number in parenthesis shows the statistical error of the numerical integration on the last digit.

The effect of the vacuum polarization can be included if one uses the running QED coupling in the SF method. The $ff\gamma$ coupling evolved by the

renormalization group equation is given by

$$g_{ff\gamma}(-t_\pm) = g_{ff\gamma}(0)\left(1 - \frac{\alpha}{3\pi}\sum_i C_i e_i^2 \log\frac{-t_\pm}{m_i^2}\Theta(-t_\pm - m_i^2)\right)^{-1}, \qquad (17)$$

where $\alpha = 1/137.036$ is the QED coupling at the zero momentum transfer, C_i the color factor, e_i the electric charge in unit of the e^+ charge, m_i the mass of the i-th fermion. The index i runs over all massive fermions. Only those fermions whose mass is greater than $-t_\pm$ are taken into account through the step function. The quark masses are chosen so as to match with the vacuum polarization in the `BDK` program. The results are shown in Table 2. The deviation from the `BDK` program is typically around 0.5%.

E_{CM} (GeV)	$\sigma_{\texttt{sf}}$ (nb)	$\sigma_{\texttt{QEDPS}}$ (nb)	$\sigma_{\texttt{BDK}}$ (nb)
20	97.5 (1)	96.9(1)	97.1(1)
40	137.8 (1)	137.1(2)	137.3(1)
100	203.3 (1)	202.2(3)	202.4(2)
200	262.6 (1)	261.2(3)	261.2(2)

Table 2: Total cross sections with the vacuum polarization. The number in parenthesis shows the statistical error of the numerical integration on the last digit.

The differential cross sections with respect to the e^- energy and angle, the CM energy of the final four-fermions and the invariant mass of the $\mu^\pm$-pair at the CM energy of 200 GeV are shown in Fig.3. The two programs give consistent distributions.

In order to check the recoiling effect of the final e^- due to the photon emission by `QEDPS`, the e^- polar angle is compared in Fig.4 between SF and `QEDPS`. The cross sections with the e^- angle between 10° and 20° are found to be 6.00(5.80) pb for `QEDPS`(SF) at the CM energy of 200 GeV. It is not surprising that the agreement becomes worse than the total cross sections, because SF includes no recoiling at all.

If a wrong energy scale of $s = (p_- + p_+)^2$ is used instead of $t_\pm$ as the energy evolution scale in the ISR tool, one may get over-estimation of the ISR effect. At the CM energy of 200 GeV, SF with the energy scale of s gives the total cross section of 257.8nb instead of 262.6nb with the correct energy scale.

3.2 Single-tagging Case

The same comparison is done for the e^--tagging case. The experimental cuts applied are:
For the e^-,

- $10^\circ < \theta_{e^-} < 170^\circ$,
- $E_{e^-} > 1$ GeV.

For the $\mu^\pm$,

- $10^\circ < \theta_{\mu^\pm} < 170^\circ$,
- $E_{\mu^\pm} > 1$ GeV,
- $M_{\mu\mu} > 1$ GeV.

The total cross sections with the above cuts at the CM-energy of 200 GeV are calculated to be 1.169 ± 0.004pb(1.13 ± 0.01pb) by `GRACE` with `QEDPS`(by `BDK`). The vacuum polarization, *i.e.* the running α, is included. This small discrepancy may come from the finite recoiling of the final e^- by the soft photon emissions in `QEDPS`. The differential cross sections are also compared in Fig.4. The results of `GRACE` with `QEDPS` are in good agreement with `BDK`.

4 Energy Scale Determination

The factorization theorem for the QED radiative corrections in the LL approximation is valid independent of the structure of the matrix element of the kernel process. Hence SF and `QEDPS` must be applicable to *any* e^+e^- scattering processes. However, the choice of the energy scale in SF and `QEDPS` is not a trivial issue. For a simple process like the two-photon process with only the multi-peripheral diagrams considered so far, the evolution energy scale could be determined by making use of the exact perturbative calculations. However, this is not always possible for more complicated processes. Hence a way to find a suitable energy scale without knowing the exact loop calculations should be established somehow.

First let us look at the general consequence of the soft photon approximation. The soft photon cross section(including both the real and the virtual

photon effects) is given by the Born cross section multiplied by some correction factor in the LL order as[14]

$$\begin{aligned}\frac{d\sigma_{soft}(s)}{d\Omega} &= \frac{d\sigma_0(s)}{d\Omega} \\ &\times \left|\exp\left[-\frac{\alpha}{\pi}\ln\left(\frac{E}{k_c}\right)\sum_{i,j}\frac{e_i e_j \eta_i \eta_j}{\beta_{ij}}\ln\left(\frac{1+\beta_{ij}}{1-\beta_{ij}}\right)\right]\right|^2, \qquad (18)\\ \beta_{ij} &= \left(1-\frac{m_i^2 m_j^2}{(p_i\cdot p_j)^2}\right)^{\frac{1}{2}}, \qquad (19)\end{aligned}$$

where m_j's(p_j's) are the mass(momentum) of j-th charged particle, k_c the maximum energy of the soft photon (boundary between soft- and hard-photons), E the beam energy, and e_j the electric charge in unit of the e^+ charge. The factor η_j is -1 for the initial particles and $+1$ for the final particles. The indices (i,j) run over all the charged particles in the initial and final states.

For the process (4) one can see that the soft-photon factor in Eq.(18) with a $(p_-\cdot q_-)$-term reproduces Eq.(16) in the LL approximation. This implies that one is able to read off the possible evolution energy scale in SF from Eq.(18) without explicit loop calculations. However, one may have a question why the energy scale $s=(p_-+p_+)^2$ does not appear in the soft-photon correction even they are included in Eq.(18). When we applied SF to the two-photon process in the previous section, we have ignored those terms which come from the photon bridged between different charged lines. This is because the contributions from the box diagrams with photon exchange between e^+ and e^- is known to be small[10]. Fortunately the infrared part of the loop correction is already included in Eq.(18) and no need to know the full form of the loop diagram. For the two-photon processes if one looks at two terms with, for example $(p_-\cdot p_+)$- and with $(q_-\cdot p_+)$-terms, the momentum of e^- is almost the same before and after the scattering($p_-\approx q_-$). Only the difference appears in $\eta_j\eta_k=+1$ for a (p_-p_+)-term and $\eta_j\eta_k=-1$ for a (q_-p_+)-term. Then these terms compensate each other after summing them up for the forward scattering which is the dominant kinematical region of this process. This is why the energy scale $s=(p_-+p_+)^2$ does not appear in the soft-photon correction despite the fact that it exists in Eq.(18).

When some experimental cuts are imposed, for example the final e^- is tagged in a large angle, this cancellation is not perfect but partial and the

energy scale s must appear in the soft-photon correction. In this case the annihilation type diagrams will also contribute to the matrix elements. Then the usual SF and `QEDPS` for the annihilation processes are justified to be used for the ISR with the energy scale s. One can check which energy scale is dominant under the given experimental cuts by numerically integrating the soft-photon cross section given by Eq.(18) over the allowed kinematical region. Thus in order to determine the energy scale it is sufficient to know the infrared behavior of the radiative process using the soft-photon factor. In some region of the phase-space two or more energy scales may be involved in the soft-photon cross section with comparable amount of contribution. In this region a simple SF and `QEDPS` are not applicable.

5 Conclusions

Two practical tools to incorporate with the QED radiative corrections are developed for non-annihilation processes by means of the structure function and the parton shower. These programs are applied to the two-photon process, $e^+e^- \to e^+e^-\mu^+\mu^-$. The results are compared with the perturbative calculation of the $O(\alpha)$ and show a good agreement.

These tools should be applicable to any non-annihilation process universally. It is demonstrated that the energy scale for the evolution, which depends on the dominant diagrams in the interested kinematical region, can be determined with the help of the well known formula of the soft photon factor. As an example we have tried a real W production in e^+e^- annihilation. The application of these tools to more complicated processes like four-fermion final state including a single-W production are left to the future publications.

References

[1] T. Kinoshita, J. Math. Phys. **3** (1962) 650,
T.D. Lee, M. Nauenberg, Phys. Rev. **B133** (1964) 1549.

[2] E.A. Kuraev, V.S. Fadin, Sov. J. Nucl. Phys. **41** (1985) 466,
G. Altarelli, G. Martinelli, in *"Physics at LEP"* J. Ellis, R. Peccei eds. CERN 86-02 (CERN, Geneva, 1986),

O. Nicrosini, L. Trentadue, Phys. Lett. **B196** (1987) 551; Z. Phys. **C39** (1988) 479,
F.A. Berends, G. Burgers, W.L. van Neerven, Nucl. Physc **B297** (1988) 429.

[3] G. Marchesini, B.R. Webber, Nucl. Phys. **B238** (1984) 1,
R. Odorico, Nucl. Phys. **B172** (1980) 157,
T Sjöstrand, Comput. Phys. Commun. **79** (1994) 503.

[4] T. Munehisa, J. Fujimoto, Y. Kurihara, Y. Shimizu, Prog. Theor. Phys. **95** (1996) 375.

[5] "ALIBABA", W. Beenakker, F.A. Berends, S.C. van der Marck, Nucl. Phys. **B349** (1991) 323,
"FERMISV" J.H. Hilgart, R. Kleiss, F. Le Diberder, Comput. Phys. Commun. **75** (1993) 191,
"UNIBAB" H. Anlauf, P. Manakos, T. Ohl, T. Mannel, H. Meinhard, H.D. Dahmen, Comput. Phys. Commun. **79** (1994) 466,
"SABSPV"M. Cacciari, G.Montagna, O. Nicrocini, F. Piccinini, Comput. Phys. Commun. **90** (1995) 301.

[6] J. Fujimoto, Y. Shimizu, T. Munehisa, Prog. Theor. Phys. **91** (1994) 333,
K. Tobimatu, in preparation.

[7] J. Fujimoto, M. Igarashi, N. Nakazawa, Y. Shimizu, K. Tobimatsu, Prog. Theor. Phys. Suppl. No.100 (1990), 1. Formulae used in the present work are given in Chapter 11.

[8] R. Odorico, Nucl. Phys. **B172** (1980) 157,
G. Marchesini, B.R. Webber, Nucl. Phys. **B238** (1984) 1.

[9] F.A. Berends, P.H. Daverveldt, R. Kleiss, Nucl. Phys. **B253** (1985) 412.

[10] W.L. van Neerven, J.A.M Vermaseren, Nucl. Phys. **B238** (1984) 73,
W.L. van Neerven, J.A.M Vermaseren, Phys. Lett. **B137** (1984) 241,
W.L. van Neerven, J.A.M Vermaseren, NIKHEF Amsterdam preprint 84-2 (1984).

[11] W. Beenakker, F.A. Berends, W.L. van Neerven, Proceedings of *"Radiative Correction for e^+e^- Collisions"*, Ed. J.H. Kühn, Springer-Verlag, Heidelberg 1989, p.3.

[12] T. Ishikawa, T. Kaneko, K. Kato, S. Kawabata, Y. Shimizu and H. Tanaka, KEK Report 92-19, 1993, The GRACE manual Ver. 1.0
and see also H. Tanaka, Comput. Phys. Commun. **58** (1990) 153
H. Tanaka, T. Kaneko and Y. Shimizu, Comput. Phys. Commun. **64**(1991) 149.

[13] S. Kawabata, Comp. Phys. Commun. **41** (1986) 127; *ibid.,* **88** (1995) 309.

[14] F. Bloch, A. Nordsieck, Phys. Rev. **37** (1937) 54,
D. R. Yennie, S. C. Frautschi, H. Suura, Ann. Phys. **13** (1961) 379.
See also S. Weinberg, "The Quantum Theory of Fields" (Cambridge University Press, New York, 1995), Section 13.

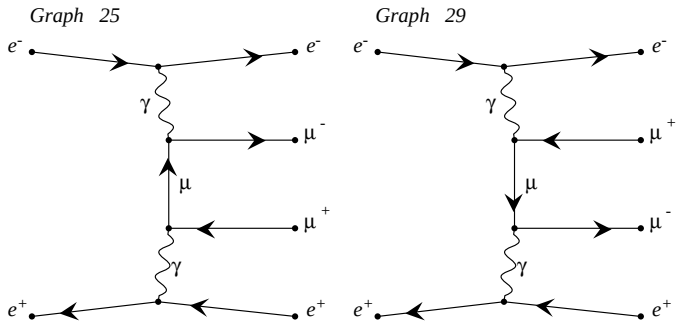

Figure 1: Multi peripheral diagrams.

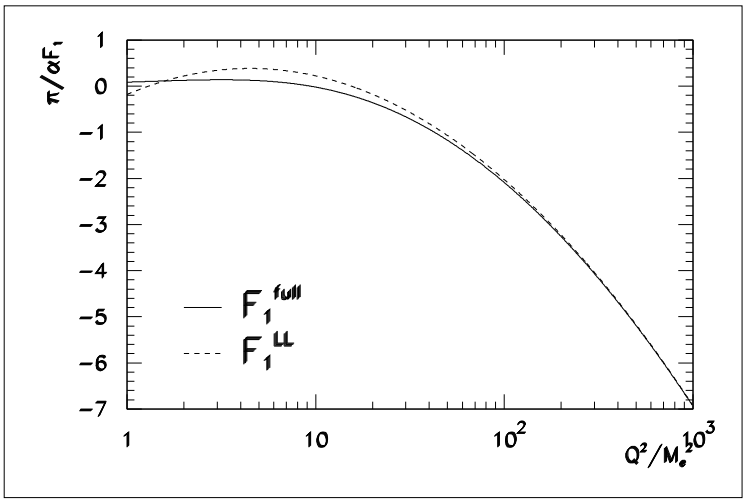

Figure 2: The exact form-factor (ReF_2) and that with LL approximation.

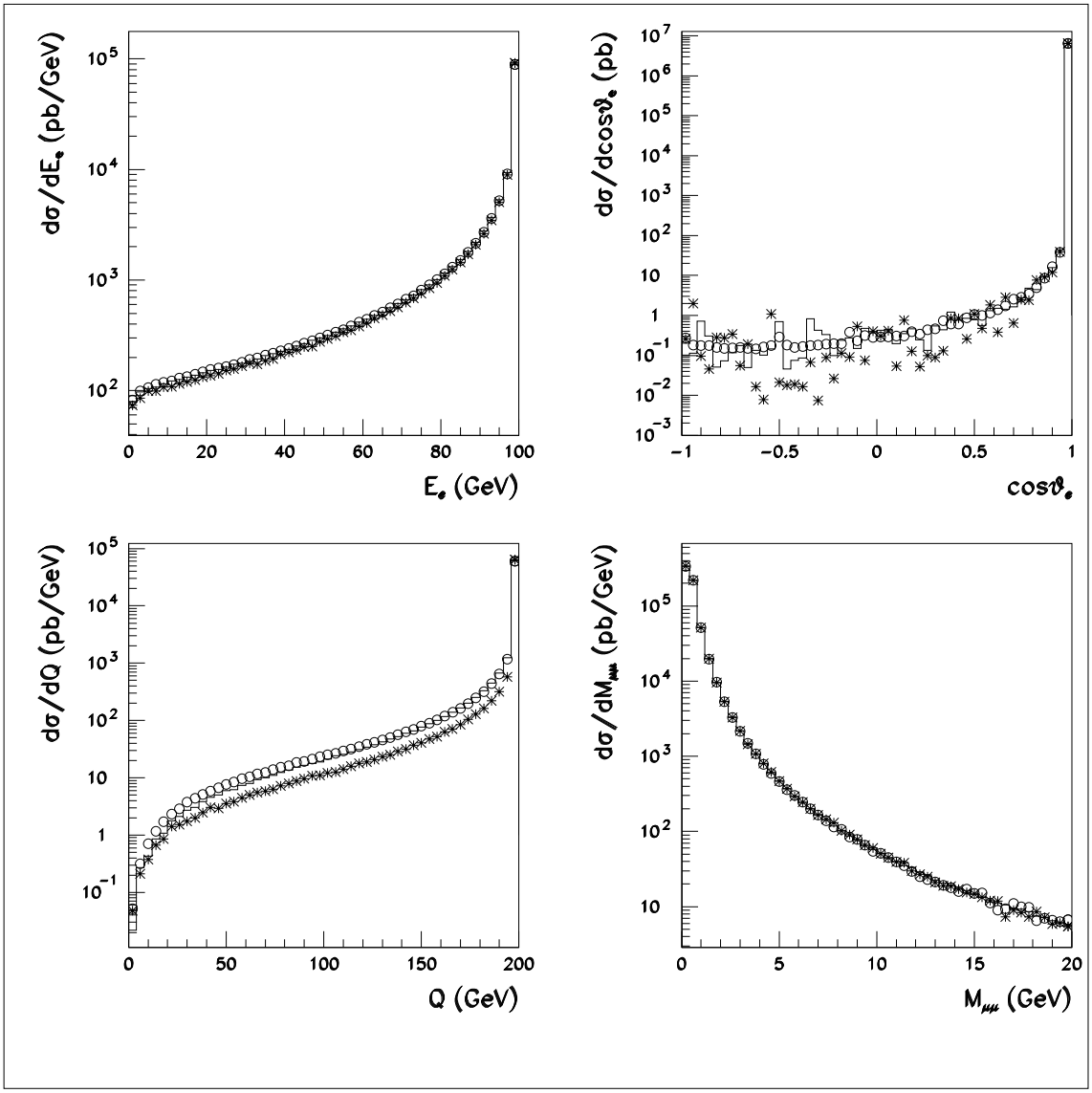

Figure 3: The differential cross sections without any experimental cuts. The solid histograms show the `GRACE-with-QEDPS` results, the stars the `GRACE-with-SF`, and the circles the `BDK` results.

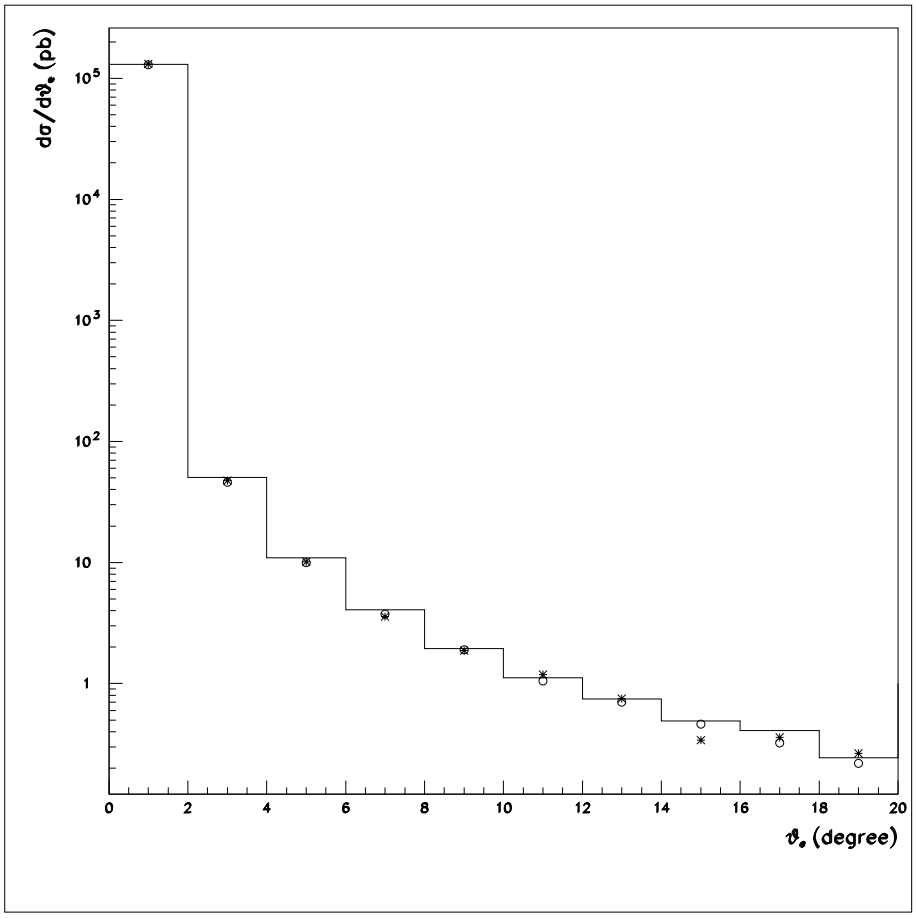

Figure 4: The e^- angle distribution with respect to the beam axis without any experimental cuts. The solid histograms show the `GRACE-with-QEDPS` results, the stars the `GRACE-with-SF`, and the circles the `BDK` results.

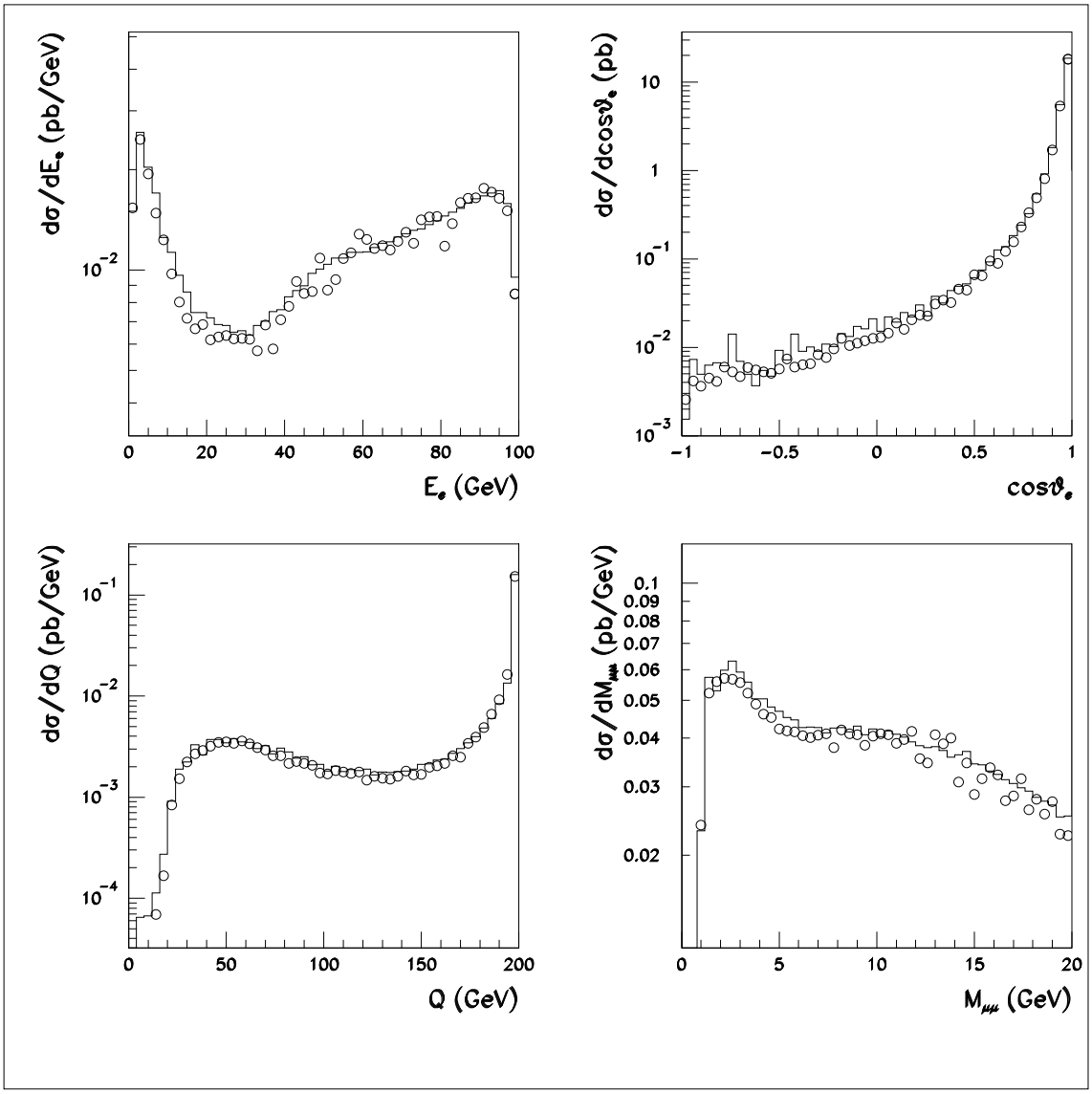

Figure 5: The differential cross sections with the e^--tagging and visible muon-pair. The solid histograms (circles) show GRACE with QEDPS (BDK) results.

Graph 21

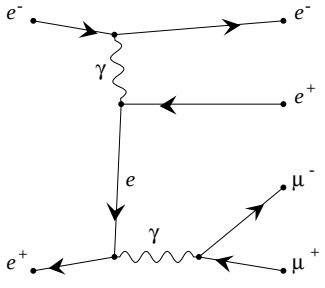

Graph 22

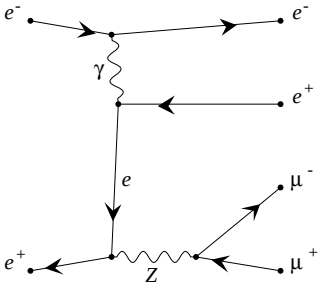

Graph 23

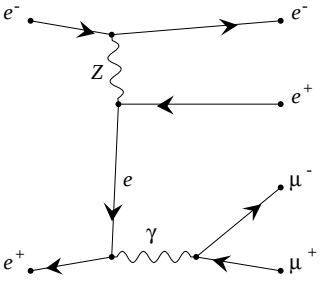

Graph 24

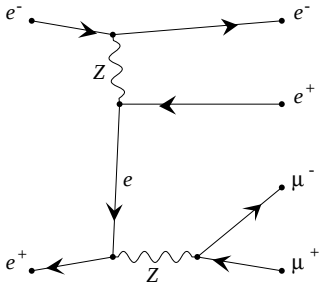

Graph 25

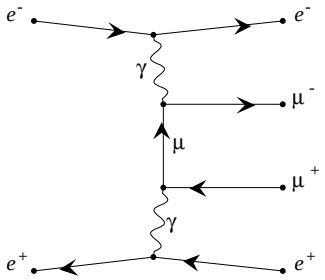

Graph 26

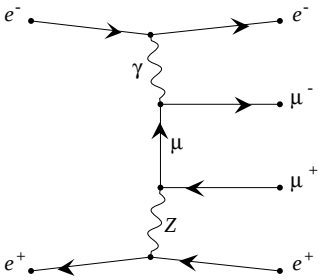

Graph 27

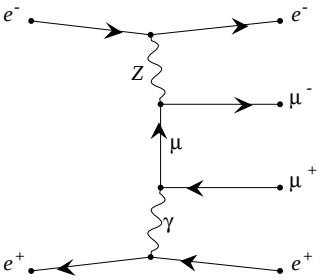

Graph 28

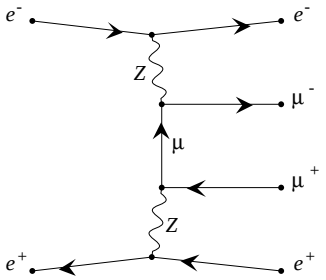

Graph 29

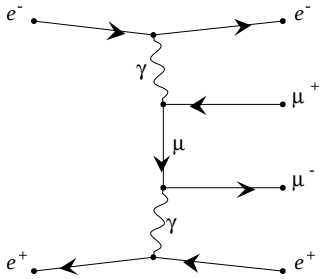

Graph 30

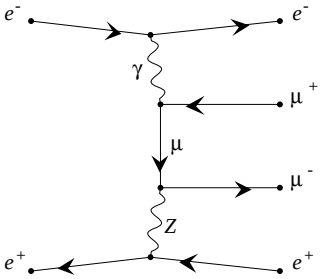

Graph 31

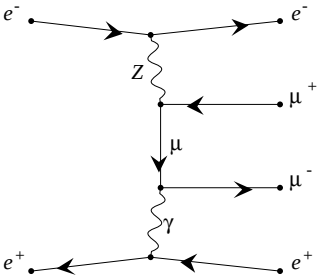

Graph 32

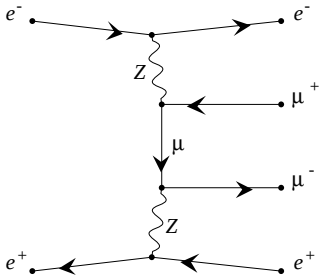

Graph 33

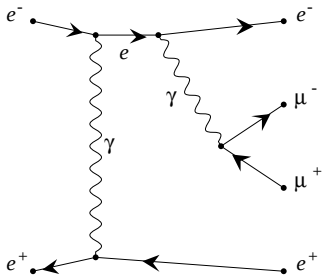

Graph 34

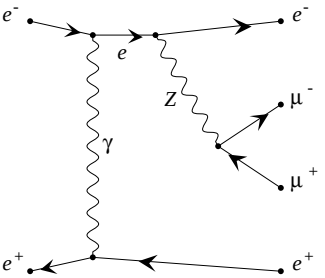

Graph 35

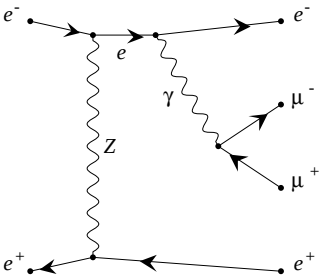

Graph 36

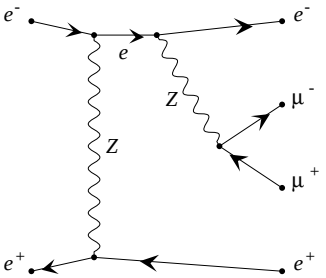

Graph 37

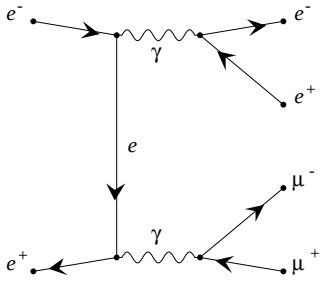

Graph 38

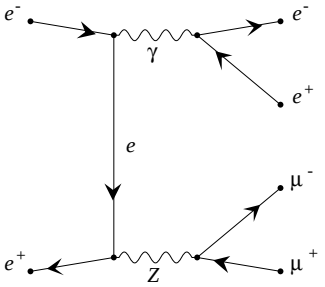

Graph 39

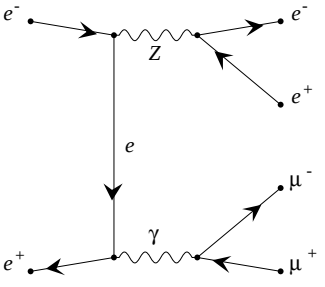

Graph 40

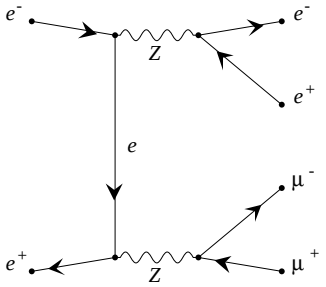

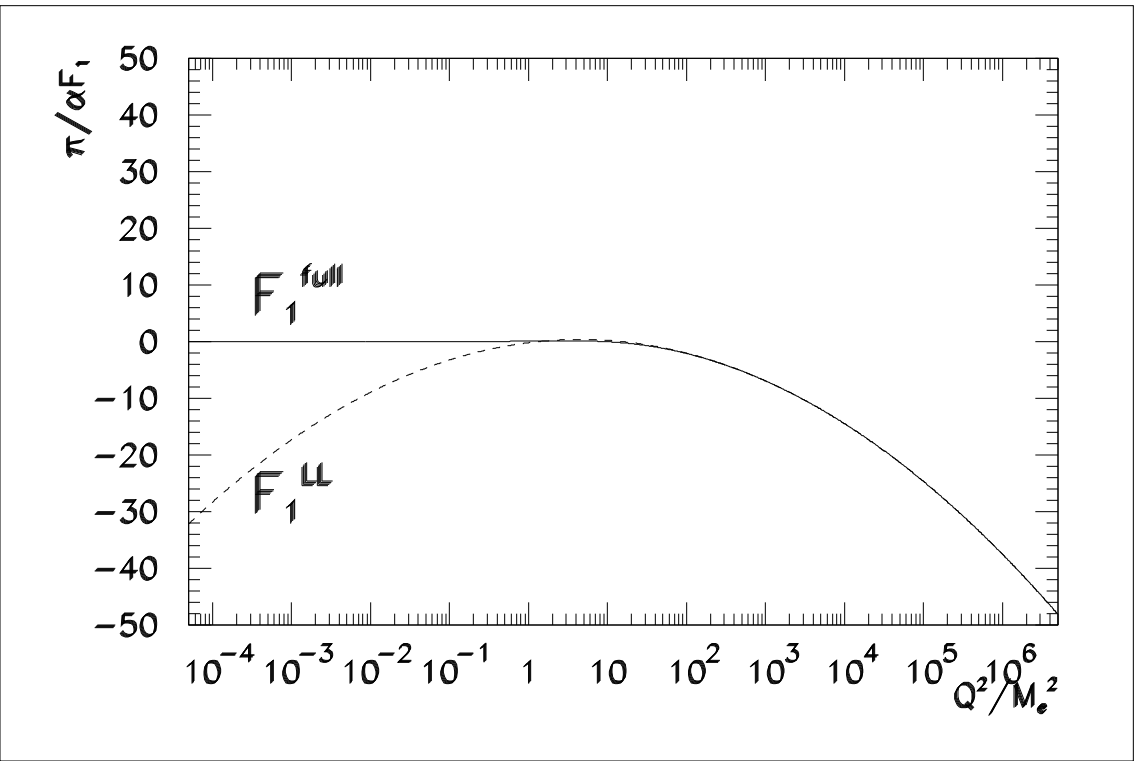
π/αF1
50
40
30
20
10
0
−10
−20
−30
−40
−50
F1full
F1LL
10−4 10−3 10−2 10−1 1 10 102 103 104 105 106
Q2/Me2

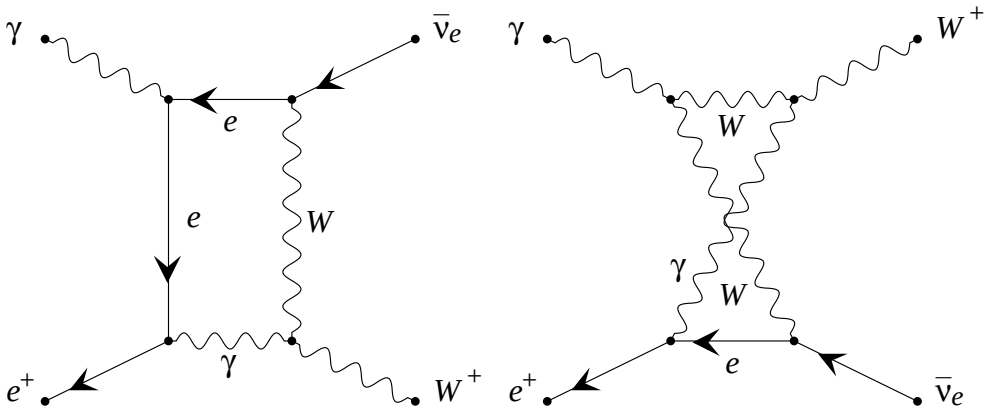
γ
$\bar{\nu}_e$
e
e
W
γ
e^+
W^+
γ
W^+
W
γ
W
e
e^+
$\bar{\nu}_e$

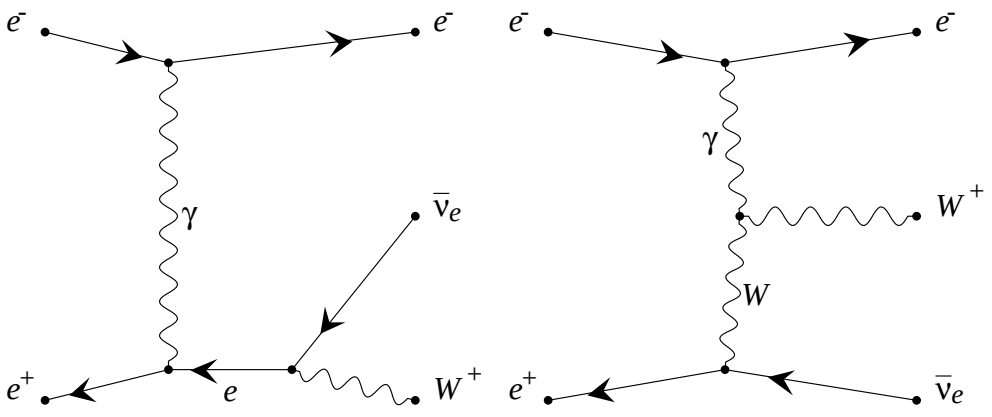
e⁻
e⁻
γ
ν̄e
e⁺
e
W⁺
e⁻
e⁻
γ
W⁺
W
e⁺
ν̄e